CHEMICAL ENGINEERING TRANSACTIONS
VOL. 69, 2018
A publication of AIDIC
The Italian Association of Chemical Engineering
Online at www.aidic.it/cet
Guest Editors: Elisabetta Brunazzi, Eva Sorensen

ISBN 978-88-95608-66-2; **ISSN** 2283-9216

Investigation of the Separation Performance of a Stripping Microchannel Device: a Model-Based Approach

Chafika Adiche

Technische Universität Darmstadt, Institute for Thermal Process Engineering, Department of Mechanical Engineering, Otto-Berndt-Straße 2, 64287 Darmstadt, Germany.
adiche@tvt.tu-darmstadt.de

In this work, a mathematical model describing the transport mechanisms in a recently developed microstripper (Adiche, 2018) was established and analytically solved. Based on this model, the overall volumetric mass transfer capacity coefficient could be estimated according to a three-resistance mass transfer model and used subsequently in combination with the HTU-NTU concept for the theoretical prediction of the separation performance of the microstripper in terms of stripping degree (Adiche, 2018). Accordingly, a sensitivity analysis of the separation performance of the device to the relevant process parameters including the liquid channel depth and the volumetric flow rates of the feed solution and carrier gas nitrogen was conducted. The comparison of the estimated stripping degrees determined in this work with those obtained experimentally from a previous work (Adiche, 2018) indicates that the developed model-based approach allows a correct prediction of the separation performance of the microstripper and constitutes therefore a useful tool towards the design optimization of the device.

1. Introduction

A liquid–vapor / gas separation microchannel device has been recently developed and successfully tested as microstripper for the removal of acetone from a dilute aqueous solution with a concentration of *5 wt %* acetone using dry nitrogen as carrier gas (Adiche, 2018). In this work, a model-based approach is presented for the theoretical investigation of the separation performance of the microstripper in terms of stripping degree. For this purpose, a mathematical model describing the transport mechanisms in the separation device including the fluid channels and the membrane contactor is established and analytically solved. Subsequently, a three-resistance mass transfer model is applied to estimate the overall volumetric mass transfer capacity coefficient. The latter is then used within a HTU-NTU approach for the prediction of the stripping degree for given liquid channel depth and volumetric flow rates of feed solution and carrier gas nitrogen. Finally, the ability of the model as predictive design tool for the microstripper is examined by comparing the estimated values of stripping degree in this work with those obtained experimentally in a previous work (Adiche, 2018).

2. Prediction of mass transfer properties in the microstripper

The overall mass transfer coefficient K_L (based on the liquid phase) in the microstripper is determined according to a three-resistance model including the resistance to mass transfer in the liquid channel, in the membrane pores and in the gas channel (Adiche, 2018) so that

$$\frac{1}{K_L} = \frac{1}{k_L} + \frac{1}{H_c k_M} + \frac{1}{H_c k_G}, \tag{1}$$

where H_c is the Henry constant for acetone in nitrogen and k_L, k_M and k_G are the individual mass transfer coefficients based on concentration difference as driving force in the liquid phase, through the membrane pores and in the gas phase, respectively.The individual mass transfer coefficient $k_{L/G}$ for the liquid / carrier gas stream can be obtained by

$$k_{L/G} = \frac{Sh_{L/G}\, D_{L/G}}{dh_{L/G}}\,, \tag{2}$$

with $Sh_{L/G}$ is the Sherwood number in the liquid / gas channel, $D_{L/G}$ the diffusion coefficient of acetone in water / nitrogen and $dh_{L/G}$ is the hydraulic diameter of the liquid / gas channel given by

$$dh_{L/G} = \frac{2\,W\,H_{L/G}}{W + H_{L/G}}\,. \tag{3}$$

In a previous work (Adiche, 2018) it was shown that for the microstripper considered in this study, the molecular diffusion is the prevailing mass transfer mechanism in the membrane pores so that the mass transfer coefficient in the membrane may be expressed as

$$k_M = \frac{\varepsilon\, D_G}{\chi\, \delta}\,, \tag{4}$$

with ε is the membrane porosity , δ the membrane thickness and χ is the membrane tortuosity.

To determine the Sherwood number in the liquid / gas channel, a two-dimensional mathematical model describing the transport mechanisms i.e. continuity, momentum, and species conservation equations, for each fluid channel of the microstripper was established [Figure 1]. The latter is based on the following assumptions:

i. the microstripper is operating under steady state, isothermal condition (ca. *23 °C*) and at atmospheric pressure,
ii. axial dispersion along the fluid flow direction and free convection at the interface between the membrane and fluid channels are neglected,
iii. laminar fully developed velocity and concentration profiles in both liquid and gas channels (Adiche, 2018), which are considered here as straight instead of meandering channels,
iv. the acetone diffusion flux *N* through the membrane pores is constant along the fluid flow direction and
v. the interface between liquid and gas phases at the membrane pore entrance is planar.

Accordingly, the Sherwood number (in analogy with Nusselt number) is expected to be constant for each fluid channel (here for a rectangular channel with constant diffusion flux through one porous side: membrane pores) (Shah and London, 1978).

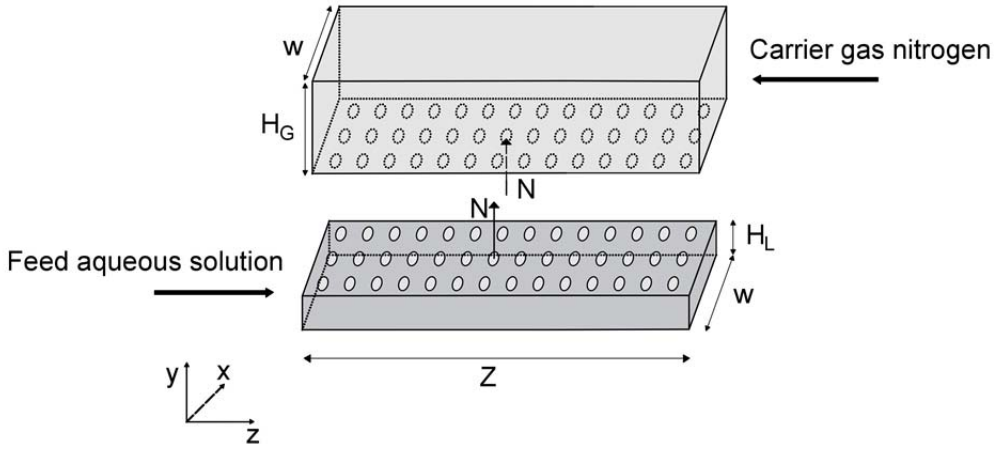

Figure 1: Model of the microstripper (exploded view) with the fluid channels are represented as straight channels instead of meandering channels (the membrane module is here omitted).

In reason of the similarity between the transport mechanisms in both fluid channels, only the equations for the liquid channel are presented in this section as follows:
The Navier-Stokes equation writes

$$\frac{\partial^2 v_{L,z}}{\partial x^2}+\frac{\partial^2 v_{L,z}}{\partial y^2}=-\frac{1}{\mu_L}\cdot\frac{dp_L}{dz}\,. \tag{5}$$

The species conservation equation for acetone is given by

$$\left(\frac{\partial^2 c_L}{\partial x^2}+\frac{\partial^2 c_L}{\partial y^2}\right)=\frac{1}{D_L}\cdot v_{L,z}(x,y)\cdot\frac{\partial c_L}{\partial z}\,, \tag{6}$$

with the mass balance equation along the flow direction writes

$$\frac{\partial c_L}{\partial z}=\frac{Na}{\langle v_{L,z}\rangle}\,, \tag{7}$$

where a is the specific interfacial area per unit volume of the wetted device estimated by

$$a=\varepsilon/H_L\,, \tag{8}$$

and $\langle v_{L,z}\rangle$ is the average velocity over the channel cross section area $W\times H_L$ defined as

$$\langle v_{L,z}\rangle=\frac{\int_0^{H_L}\int_0^{W} v_{L,z}\,dxdy}{\int_0^{H_L}\int_0^{W} dxdy}\,, \tag{9}$$

and finally the acetone diffusion flux N is given by

$$N=k_L\left(c_L^B-c_L^M\right), \tag{10}$$

with c_L^B and c_L^M are the average concentrations of acetone in the liquid phase over the channel cross section area $W\times H_L$ and at the membrane pore entrance along the length W, respectively.

The boundary conditions for the velocity field are given by

$$v_{L,z}\big|_{x=0}=0\,,\ v_{L,z}\big|_{x=W}=0\,,\ v_{L,z}\big|_{y=0}=0\,,\ v_{L,z}\big|_{y=H_L}=0\,, \tag{11}$$

and those for the concentration field by

$$\left.\frac{\partial c_L}{\partial x}\right|_{x=0}=0\,,\ \left.\frac{\partial c_L}{\partial x}\right|_{x=W}=0\,,\ \left.\frac{\partial c_L}{\partial y}\right|_{y=0}=0 \text{ and } \left.\frac{\partial c_L}{\partial y}\right|_{y=H_L}=-\frac{N}{D_L}\,,$$

with $0\le x\le W$ and $0\le y\le H_L$. (12)

The dimensionless variables are defined as follows

$$\xi=\frac{x}{W}\,,\ \eta=\frac{y}{W}\,,\ \text{with } 0\le\xi\le 1 \text{ and } 0\le\eta\le\beta_L=\frac{H_L}{W}\,,\ \text{with } \beta_L \text{ is the aspect ratio of the liquid channel,} \tag{13.a}$$

$$u_{L,\varsigma}(\xi,\eta)=\frac{v_{L,z}(x,y)}{\frac{W^2}{\mu_L}\cdot\frac{\Delta p_L}{Z}}\,, \tag{13.b}$$

and $\omega_L=\dfrac{c_L-c_{L,in}}{Ndh_L/D_L}$, with $c_{L,in}$ is the inlet molar concentration of acetone in the feed solution. (13.c)

Accordingly, the dimensionless Navier-Stokes equation and the related boundary conditions write

$$\frac{\partial^2 u_{L,\varsigma}(\xi,\eta)}{\partial\xi^2}+\frac{\partial^2 u_{L,\varsigma}(\xi,\eta)}{\partial\eta^2}=-1\,,\ u_{L,\varsigma}\big|_{\xi=0}=0\,,\ u_{L,\varsigma}\big|_{\xi=1}=0\,,\ u_{L,\varsigma}\big|_{\eta=0}=0\,,\ u_{L,\varsigma}\big|_{\eta=\beta_L}=0\,. \tag{14}$$

The solution of Eqs. (14) is obtained analytically (Spiga and Morini, 1994) and is given by

$$u_{L,\varsigma}(\xi,\eta)=\frac{16\beta_L^{\,2}}{\pi^4}\sum_{n\,odd}^{\infty}\sum_{m\,odd}^{\infty}\frac{\sin(n\pi\xi)\sin\left(m\pi\dfrac{\eta}{\beta_L}\right)}{nm\left(\beta_L^{\,2}n^2+m^2\right)}\,. \tag{15}$$

Combining Eqs. (9) with (13.b) and (15) gives rise to

$$\langle v_{L,z}\rangle=\frac{64\,\beta_L^{\,2}}{\pi^6}\cdot\frac{W^2\Delta P_L}{\mu_L Z}A_L\,,\ \text{with } A_L=\sum_{n\,odd}^{\infty}\sum_{m\,odd}^{\infty}\frac{1}{n^2m^2\left(\beta_L^{\,2}n^2+m^2\right)}\,. \tag{16}$$

Furthermore, the dimensionless species conservation equation for acetone with the related boundary conditions are given by

$$\frac{\partial^2 \omega_L}{\partial \xi^2} + \frac{\partial^2 \omega_L}{\partial \eta^2} = \frac{\varepsilon(1+\beta_L)}{2{\beta_L}^2} \cdot \frac{1}{\langle v_{L,z} \rangle} \cdot \frac{W^2 \Delta P_L}{\mu_L Z} u_{L,\varsigma}(\xi,\eta) \tag{17.a}$$

$$\text{and } \left.\frac{\partial \omega_L}{\partial \xi}\right|_{\xi=0} = 0,\ \left.\frac{\partial \omega_L}{\partial \xi}\right|_{\xi=1} = 0,\ \left.\frac{\partial \omega_L}{\partial \eta}\right|_{\eta=0} = 0,\ \left.\frac{\partial \omega_L}{\partial \eta}\right|_{\eta=\beta_L} = -\frac{(1+\beta_L)}{2\beta_L}. \tag{17.b}$$

Combining Eqs. (17.a) with (15) and (16) results in

$$\frac{\partial^2 \omega_L}{\partial \xi^2} + \frac{\partial^2 \omega_L}{\partial \eta^2} = \frac{\varepsilon(1+\beta_L)}{2{\beta_L}^2} \cdot \frac{\pi^2}{4A_L} \cdot \sum_{n\,odd}^{\infty} \sum_{m\,odd}^{\infty} \frac{\sin(n\pi\xi)\sin\left(m\pi\frac{\eta}{\beta_L}\right)}{nm\left({\beta_L}^2 n^2 + m^2\right)}. \tag{18}$$

The concentration profile is then determined (Matlab®) by solving the mass balance equation (Eq. (18)) according to the analytical method developed in the work of Spiga and Morini (1996) for the determination of the temperature profile and the Nusselt number in rectangular ducts for H2 boundary conditions. Subsequently, the Sherwood number is obtained by combining Eq. (2) with Eqs. (10) and (13.c) such that

$$Sh_L = \frac{1}{\omega_L^B - \omega_L^M}, \tag{19}$$

with the average dimensionless acetone concentration in the liquid channel ω_L^B is given by

$$\omega_L^B = \frac{\int_0^{\beta_L}\int_0^1 u_{L,\varsigma}\omega_L \, d\xi \, d\eta}{\int_0^{\beta_L}\int_0^1 u_{L,\varsigma} \, d\xi \, d\eta}, \tag{20}$$

and the average dimensionless liquid acetone concentration at the membrane pore entrance ω_L^M writes

$$\omega_L^M = \int_0^1 \omega_L(\xi,\beta_L)\, d\xi. \tag{21}$$

Once the Sherwood numbers for the liquid and carrier gas streams have been determined, the respective individual mass transfer coefficients $k_{L/G}$ can be obtained using Eq. (2). Subsequently, combining Eqs. (1) and (4) provides the overall mass transfer coefficient K_L. The latter is then multiplied by the estimated specific interfacial area for mass transfer a (Eq. (8)); providing thereby the predicted overall volumetric mass transfer capacity coefficient $(K_L a)_{predic}$.

3. Results and discussion

The estimated overall volumetric mass transfer capacity coefficient $(K_L a)_{predic}$ in the microstripper was determined for each tested liquid channel depth (*100* and *300 µm*) according to the model-based approach presented in Section 2. For this purpose, the relevant thermodynamic and transport properties of acetone were used [Table 1]. In addition, a membrane tortuosity χ equal to *2* was considered.

Table 1: Thermodynamic and transport properties of acetone in the microstripper (Adiche, 2018)

Property	Value
H_c (kmol/m^3/kmol/m^3)	1.3 10^{-3}
D_L (m^2/sec)	1.2 10^{-9}
D_G (m^2/sec)	1.3 10^{-5}

Table 2 shows that for both liquid channel depths, the predicted overall volumetric mass transfer capacity coefficients underestimate the corresponding values determined experimentally in the previous work (Adiche, 2018) with however a higher extent for the greater liquid channel depth (aspect ratio). This discrepancy may be attributed to the restriction of the elaborated model to fully developed velocity and concentration profiles in straight fluid channels with constant acetone diffusion flux along the fluid flow direction. So that the entrance-length effects as well as the developing regions, which may occur in the meandering fluid channels of the microstripper are here not considered. Consequently, the developed model provides a minimum Sherwood number in each fluid channel (Clark and Kays, 1952); resulting therefore in a minimum overall mass transfer

coefficient in the microstripper. A further possible cause of this discrepancy is the actually curved interface between the liquid and vapor / gas phases at the membrane contactor entrance due to the prevailing surface tension between the feed solution and the hydrophobic membrane contactor (Probstein, 2003). In this work however the interface between the liquid and vapor / gas phases is assumed to be planar. That results in underestimating the specific interfacial area *a* because of a smaller surface area for the wetted device as compared to that expected for a curved interface; leading consequently to lower values of predicted overall volumetric mass transfer capacity coefficients as compared to those obtained experimentally.

Table 2: Comparison between the experimental (Adiche, 2018) and predicted values of overall mass transfer coefficients in the microstripper

H_L (µm)	$(K_La)_{exp}$ (s^{-1})(Adiche, 2018)	$(K_La)_{predic}$ (s^{-1}) (this work)	$[(K_La)_{predic} - (K_La)_{exp}]/ (K_La)_{exp}$ (%)
100	0.091	0.062	-31.9
300	0.018	0.011	-38.9

Further investigations were carried out to examine the impact of varying alternatively the liquid and carrier gas flow rate on the stripping degree of the microstripper for each tested liquid channel depth by using the corresponding predicted value of overall mass transfer coefficient determined in this work [Table 2]. The predicted stripping degree is therefore determined according to the HTU-NTU concept (Adiche, 2018) using the following relationship

$$\sigma_{predic} = 1 - \frac{S-1}{S\,Exp\left(\dfrac{(K_La)_{predic}\;W\,H_L\,Z\,(S-1)}{S\,Q_L}\right)-1}, \qquad (22)$$

where Q_L and S are the liquid volumetric flow rate and the stripping factor, respectively.

Figure 2 shows that for the two tested liquid channel depths, similar trends were found for the variation of both experimental (σ_{exp}) and predicted (σ_{predic}) stripping degrees with the liquid residence time. For H_L = *100 µm*, the relative deviation of σ_{predic} with respect to σ_{exp} varies between *-2.0 %* and *-21.4 %*, increasing with the decrease of the liquid residence time. Similarly for H_L = *300 µm*, the relative deviation of σ_{predic} to σ_{exp} increases with decreasing the liquid residence time, but in this case in a range between *-10.0 %* and *-29.3 %*. This discrepancy can be well explained by the lower predicted overall volumetric mass transfer capacity coefficients as compared to the respective experimental values with however a higher extent for the greater liquid channel depth.

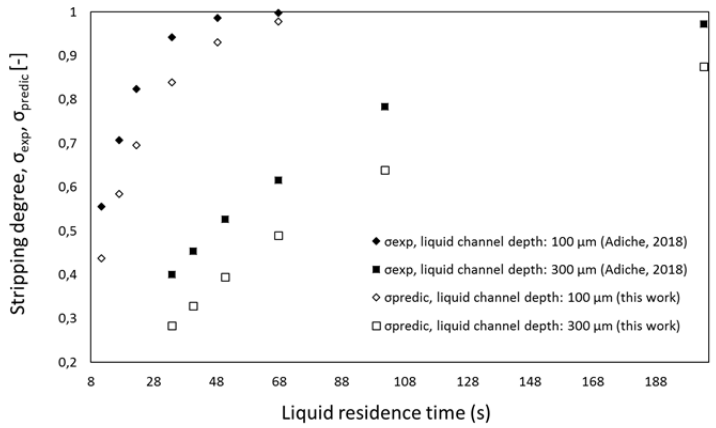

Figure 2: Influence of the liquid residence time on the experimental and predicted stripping degrees for a carrier gas flow rate of 163 ml /min.

Figure 3 illustrates the variation of both experimental and predicted stripping degrees with the carrier gas flow rate. Here also, it is shown that for each tested H_L both curves present similar trends with higher values for σ_{exp} as compared to the respective $\sigma_{predict}$. However, it is worth noticing that contrary to the results presented in the previous section [see also Figure 2], the relative deviation of σ_{predic} with respect to σ_{exp} is here hardly affected by the variation of the carrier gas flow rate, with average values of *-6.5 %* and *-25.9 %* for H_L equal to *100 µm* and *300 µm*, respectively.

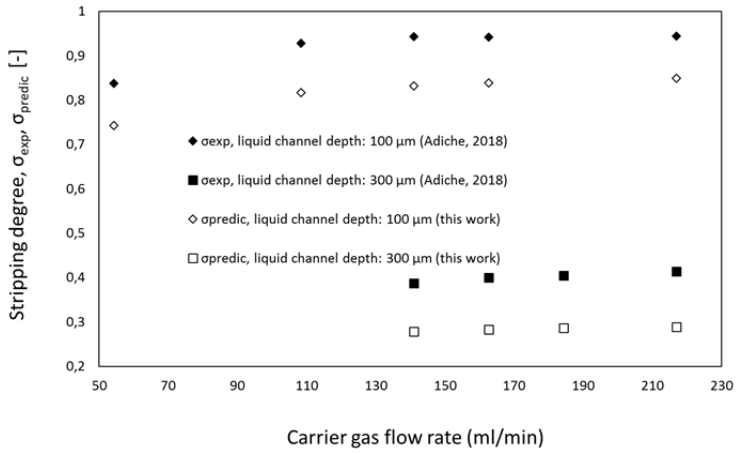

Figure 3: Influence of the carrier gas flow rate on the experimental and predicted stripping degrees for a liquid residence time of 34 s.

4. Conclusion

The comparison between the estimated stripping degrees determined in this work using a model-based approach and those obtained experimentally from a previous work (Adiche, 2018) reveals that the developed model allows a qualitative prediction of the impact of both miniaturization (with decreasing the liquid channel depth) and variation of the liquid and carrier gas flow rates on the separation performance of the microstripper. The accuracy of the model in predicting the stripping degree was found strongly sensitive to the liquid flow rate (liquid residence time) and to the liquid channel depth while barely affected by the carrier gas flow rate, with the best value achieved for a liquid channel depth of *100 µm* and a liquid residence time of *68 s* corresponding to a relative deviation of σ_{predic} with respect to σ_{exp} of *-2.0 %*.

References

Adiche C., 2018, Stripping of acetone from water in a microchannel device, Separation and Purification Technology, 199, 105-113.

Clark S. H. and Kays W. M., 1952, Laminar-Flow Forced Convection in Rectangular Tubes, Transactions of the ASME, 859-866.

Curcio E. and Drioli E., 2005, Membrane distillation and related operations-A review, Separation and Purification Reviews, 34, 1, 35-86.

McCabe W. L., Smith J. C., Harriott P., 2005, Unit Operations of chemical engineering, seventh Edition, McGraw Hill International Edition.

Probstein R. F., 2003, Physicochemical Hydrodynamics, An Introduction, Second Edition, John Wiley & Sons, Inc., Hoboken, New Jersey.

Shah R.K and London A.L, 1978, Laminar Flow Forced Convection in Ducts, Advanced Heat Transfer, Academic Press, New York.

Spiga M. and Morini G. L., 1994, A symmetric solution for velocity profile in laminar flow through rectangular ducts, International Communications in Heat and Mass Transfer, 21, 4, 469-475.

Spiga M. and Morini G. L., 1996, Nusselt numbers in laminar flow for H2 boundary conditions, Int. J. Heat Mass Transfer, 39, 6, 1165-1174.